第 35 卷第 8 期 无 机 化 学 学 报 Vol.35 No.8
2019 年 8 月 CHINESE JOURNAL OF INORGANIC CHEMISTRY 1340-1348

苯并咪唑基 Ir(Ⅲ)配合物的合成、结构和发光行为的调控或转换

芮 凯 吴石山 曹登科*
(南京大学化学化工学院,南京 210093)

摘要：合成了 2 个新的铱配合物[Ir(ppy)(qbiH)]NO_3 (**1**·NO_3)和[Ir(ppy)(qbi)] (**2**)。晶体结构分析表明,配合物 **1**·NO_3 和 **2** 中的 $[Ir(ppy)_2]^+$单元分别与苯并咪唑基的中性配体 qbiH 与阴离子配体 qbi^-螯合。在溶液以及在固态条件下,2 个配合物表现出明显不同的发光行为。**1**·NO_3 和 **2** 在 CH_2Cl_2 溶液中的磷光发射波长分别为 581 和 574 nm。在固态,**1**·NO_3 和 **2** 分别发红色(616 nm)与桔色(598 nm)的磷光。有趣的是,**1**·NO_3 和 **2** 在 Et_3N 或 TFA 蒸汽的作用下,表现出红光发射与桔光发射之间的转换,这是因为它们的配体 qbiH 和 qbi^-发生了酸碱诱导的结构转换。此外,还讨论了配合物 **1**·NO_3 和 **2** 的结构与发光行为之间的关系。

关键词：铱配合物；晶体结构；光发射的转换或调控
中图分类号：O614.81+2 **文献标识码**：A **文章编号**：1001-4861(2019)08-1340-09
DOI:10.11862/CJIC.2019.156

Benzoimidazole-Based Cyclometalated Ir(Ⅲ) Complexes: Syntheses, Structures and Luminescence Modulation/Switching

RUI Kai WU Shi-Shan CAO Deng-Ke*
(*School of Chemistry and Chemical Engineering, Nanjing University, Nanjing* 210093, *China*)

Abstract: Two iridium complexes [Ir(ppy)(qbiH)]NO_3 (**1**·NO_3) and [Ir(ppy)(qbi)] (**2**) have been synthesized. Their crystal structures indicate that an $[Ir(ppy)_2]^+$ unit is chelated by a neutral benzoimidazole-based ligand qbiH in **1**·NO_3, while anion ligand qbi^- in **2**. The different deprotonation degrees of ligands qbiH and qbi^- in the two complexes lead to their clear differences in luminescence both in solution and in solid state. Complexes **1**·NO_3 and **2** in CH_2Cl_2 show the emissions at 581 and 574 nm, respectively. In solid state, a red emission at 611 nm was observed for **1**·NO_3, while an orange emission at 598 nm for **2**. It is interesting that both **1**·NO_3 and **2** in solid state exhibited luminescence switching between red emission and orange emission, upon meeting Et_3N/TFA vapor. This is due to the acid/base-induced structural interconversion between ligand qbiH and ligand qbi^- in complexes **1**·NO_3 and **2**. Moreover, we discuss the relationship between structure and luminescence for **1**·NO_3 and **2**. CCDC: 1907283, **1**·NO_3; 1907284, **2**.

Keywords: iridium complex; crystal structure; luminescence modulation/switching

0 Introduction

It is well known that an imidazole unit can coordinate to a metal ion through its neutral -N= donor or deprotonated -N^-- donor. In this regard, some cyclometalated Ir(Ⅲ) complexes incorporate imidazole units, leading to various structures and the related switching of photophysical properties. For example,

收稿日期:2019-04-04。收修改稿日期:2019-04-26。
国家自然科学基金(No.21871134)资助项目。
*通信联系人。E-mail:dkcao@nju.edu.cn;会员登记号:S06N0040M1202。

Williams group firstly reported the proton-switchable behavior from a pair of benzoimidazole-based cyclometalated Ir(Ⅲ) complexes $[Ir(ppy)_2(pybzH)]PF_6$ and $[Ir(ppy)_2(pybz)]$ (Scheme S1)[1], in which ligands pybzH and $pybz^-$ coordinate with Ir(Ⅲ) ions through -N=donor and deprotonated $-N^-$- donor, respectively. It was found that the two complexes in CH_2Cl_2 revealed structural interconversion upon addition of acid/base (i.e. proton-switchable behavior, Scheme S1), resulting in luminescence switching between the emission at 521 nm from $[Ir(ppy)_2(pybzH)]PF_6$ and the emission at 496 nm from $[Ir(ppy)_2(pybz)]$. After this report, the other imidazole/benzoimidazole-based $[Ir(C^N)_2(N^N)]^+$ complexes were designed and synthesized[2-6], in which the acid/base-induced transition of coordination mode between -N= mode and $-N^-$- mode resulted in the significant variations in electronic absorption spectra[3], luminescence intensity[4-5], and emission color[6].

Recently, our group reported complexes [Ir(dfppy)(qbiH)]PF_6 (**1F·PF$_6$**) and [Ir(dfppy)(qbi)] (**2F**) (Scheme 1)[6], in which an $\{Ir(dfppy)_2\}^+$ unit is chelated by a benzoimidazole-based neutral ligand qbiH using the coordination mode N^N in **1F·PF$_6$**, while anion ligand qbi^- using the coordination mode N^N^- in **2F**. Their distinct structures result in the significant differences in luminescence, strong emission at 558 nm for **1F·PF$_6$** in CH_2Cl_2 while weak emission at 546 nm for **2F**. Upon addition of NEt_3/TFA, the two complexes can switch their luminescence between strong emission at 558 nm and weak emission at 546 nm, due to their acid-/base-induced structural interconversion between the protonation state and the deprotonation state of qbiH ligand. We synthesized complexes $[Ir(ppy)(qbiH)]NO_3$ (**1·NO$_3$**) and [Ir(ppy)(qbi)] (**2**), which incorporate cyclometalated ligand ppy^- instead of the $dfppy^-$ ligands in the reported complexes **1F·PF$_6$** and **2F** (Scheme 1). The aims of this study mainly include the below two aspects. (i) We explore the influence of ligands ppy^- on the structures and associated luminescence of complexes **1·NO$_3$** and **2**. (ii) The neighboring molecules in both **1F·PF$_6$** and **2F** stack through $\pi\cdots\pi$ interactions (Fig.S1 and S2), due to the incorporation of some fluorine substituents[7]. In contrast, complexes **1·NO$_3$** and **2** without any fluorine substituent are expected to be lack of inter-molecular $\pi\cdots\pi$ stacking interactions. The resultant loose packing structures of both **1·NO$_3$** and **2** would facilitate their possible solid-state luminescence switching. Herein, we discuss the structures and luminescence modulation/switching of **1·NO$_3$** and **2**.

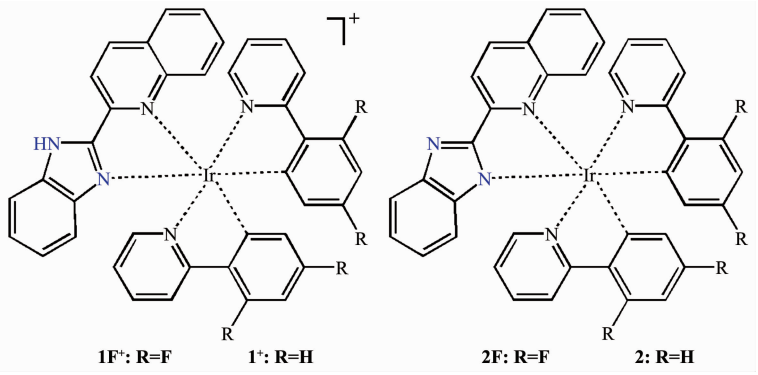

Scheme 1　Molecular structures of cations **1F**$^+$ and **1**$^+$, and complexes **2F** and **2**

1　Experimental

1.1　Materials and physical measurements

Compounds qbiH and $[Ir(ppy)_2Cl]_2$ were prepared according to the literature methods[6,8]. All other reagents were commercially available and used without further purification. Elemental analyses were performed on a Perkin Elmer 240C elemental analyzer. The IR spectra were obtained as KBr disks on a VECTOR 22 spectrometer. The ^{1}H NMR spectra were recorded at room temperature with a 400 MHz BRUKER spectrometer. UV-Vis absorption spectra were measured on a

Cary 100 spectrophotometer. The luminescence spectra at room temperature and at 77 K were measured on a Hitachi F-4600 fluorescence spectrometer. The luminescence lifetimes of **1·NO$_3$** and **2** both in CH_2Cl_2 and in solid state were measured at room temperature on a HORIBA FL-3 Spectrofluorometer with a 374 nm LED pulsed from a NanoLED resource. The photoluminescence quantum yields of **1·NO$_3$** and **2** in CH_2Cl_2 were measured by using a relative method by comparing with a standard, a solution of quinine sulfate in 0.5 mol·L^{-1} H_2SO_4 (Φ=54.6%, λ_{ex}=366 nm)[9]. The quantum yields of these complexes in the solid state were measured at room temperature on a HORIBA FL-3 spectrofluorometer.

1.2 Synthesis of [Ir(ppy)(qbiH)]NO$_3$ (1·NO$_3$)

A mixture of $[Ir(ppy)_2Cl]_2$ (0.15 mmol, 0.161 1 g), qbiH (0.3 mmol, 0.073 5 g), CH_2Cl_2 (12 mL) and CH_3OH (12 mL) was heated in an oil bath (50 ℃) under argon for one day, and then was evaporated under vacuum. To a solution of the obtained residue in CH_2Cl_2 (30 mL) was added a solution of $AgNO_3$ (0.6 mmol, 0.102 0 g) in CH_3CN (10 mL), and this mixture was stirred at room temperature overnight. After removing the resultant AgCl, the filtrate was evaporated. The residue was dissolved in a mixture of CH_2Cl_2 (40 mL) and H_2O (15 mL). The CH_2Cl_2 layer was separated and evaporated. The resultant solid was purified through silica column chromatography using CH_3OH-CH_2Cl_2 ($V_{CH_3OH}/V_{CH_2Cl_2}$=0~0.01) solution, obtaining orange-red solid (Fig.S3) with a yield of 194.4 mg (80% based on $[Ir(ppy)_2Cl]_2$). Anal. Calcd. for $C_{38}H_{27}N_6O_3Ir$(%): C, 56.50; H, 3.37; N, 10.40. Found(%): C, 56.57; H, 3.63; N, 10.61. IR (KBr, cm^{-1}): 3 444(w), 3 043(w), 2 923(w), 2 853(w), 1 604(s), 1 583(m), 1 562(w), 1 520(m), 1 477(s), 1 420(m), 1 384(s), 1 338(m), 1 321 (s), 1 267 (m), 1 227 (w), 1 161 (w), 1 116(w), 1 062(w), 1 030(w), 993(w), 873(w), 842(w), 793(w), 756(s), 731(s), 630(w), 438(w). ^{1}H NMR (400 MHz, $CDCl_3$): δ 5.91 (d, *J*=8.4 Hz, 1H), 6.23 (d, *J*=7.6 Hz, 1H), 6.48 (d, *J*=7.2 Hz, 1H), 6.83~6.91 (m, 4H), 6.96~7.05 (m, 2H), 7.10 (t, *J*=7.4 Hz, 1H), 7.19~7.22 (m, 2H), 7.44~7.48 (m, 2H), 7.58~7.89 (m, 9H), 8.16 (d, *J*=7.6 Hz, 1H), 8.51 (d, *J*=6.4 Hz, 1H) and 9.12 (broad, 1H) (5.91~7.22 and 7.44~9.12: total 26H from two ppy$^-$ units and one qbiH ligand).

1.3 Synthesis of [Ir(ppy)(qbi)] (2)

A mixture of $[Ir(ppy)_2Cl]_2$ (0.15 mmol, 0.161 1 g), qbiH (0.3 mmol, 0.073 5 g), K_2CO_3 (0.6 mmol, 0.082 8 g), CH_2Cl_2 (12 mL) and CH_3OH (12 mL) was heated in an oil bath (50 ℃) under argon for one day. After evaporation under vacuum, the resultant residue was dissolved in a mixture of CH_2Cl_2 (30 mL) and H_2O (10 mL). The CH_2Cl_2 layer was separated, dried with $MgSO_4$, and filtered. The filtrate was evaporated under vacuum. The resultant solid was purified through silica column chromatography using CH_3OH-CH_2Cl_2 ($V_{CH_3OH}/V_{CH_2Cl_2}$=0~0.005) solution, obtaining an orange-yellow solid (Fig.S3) with a yield of 181 mg (81% based on $[Ir(ppy)_2Cl]_2$). Anal. Calcd. for $C_{38}H_{26}N_5Ir$(%): C, 61.27; H, 3.52; N, 9.40. Found(%): C, 61.42; H, 3.84; N, 9.40. IR (KBr, cm^{-1}): 3 420 (w), 3 047(w), 2 924(w), 1 604(m), 1 583(w), 1 561(w), 1 521(w), 1 477 (s), 1 338(w), 1 321(w), 1 267(w), 1 161(w), 1 116(w), 1 062(w), 1 030(w), 866(w) and 755(w). ^{1}H NMR (400 MHz, $CDCl_3$): δ 5.86 (d, *J*=8.4 Hz, 1H), 6.26 (d, *J*=8.4 Hz, 1H), 6.57 (d, *J*=8.4 Hz, 1H), 6.67~6.73 (m, 3H), 6.85 (t, *J*=8.2 Hz, 1H), 6.93~7.00 (m, 2H), 7.05 (t, *J*=8.0 Hz, 2H), 7.13 (t, *J*=8.0 Hz, 1H), 7.34~7.40 (m, 2H), 7.49 (t, *J*=8.0 Hz, 1H), 7.56 (t, *J*=8.0 Hz, 1H), 7.61~7.67 (m, 2H), 7.72~7.75 (m, 2H), 7.80 (d, *J*=8.0 Hz, 1H), 7.84 (d, *J*=8.0 Hz, 1H), 7.91 (d, *J*=6.4 Hz, 1H), 8.12 (d, *J*=8.8 Hz, 1H), 8.28 (d, *J*=8.4 Hz, 1H) and 8.80 (d, *J*=8.8 Hz, 1H) (5.86~7.13 and 7.34~8.88: total 26H from two ppy$^-$ units and one qbi$^-$ ligand).

1.4 X-ray crystallographic studies

The single crystals of **1·NO$_3$** and **2** were grown from the corresponding CH_2Cl_2-CH_3OH solution. Single crystals of dimensions 0.21 mm×0.13 mm×0.10 mm for **1·NO$_3$**, and 0.18 mm×0.15 mm×0.11 mm for **2** were used for structural determination on a Bruker SMART APEX CCD diffractometer using graphite-monochromated Mo *Kα* radiation (λ=0.071 073 nm) at room temperature. A hemisphere of data were collected in the θ range of 1.50°~26.00° for **1·NO$_3$**, and 1.70°~28.24° for **2** using a narrow-frame method with scan widths of 0.30° in and an exposure time of 10 s per

frame. Numbers of observed and unique reflections are 48 567 and 6 096 (R_{int}=0.037 1) for **1·NO$_3$**, and 21 076 and 7 412 (R_{int}=0.0430) for **2**, respectively. The data were integrated using the Siemens SAINT program[10], with the intensities corrected for Lorentz factor, polarization, air absorption, and absorption due to variation in the path length through the detector faceplate. Multi-scan absorption corrections were applied. The structures were solved by direct methods and refined on F^2 by full matrix least squares using SHELXTL[11-12]. All the non-hydrogen atoms were located from the Fourier maps, and were refined anisotropically. All H atoms were refined isotropically, with the isotropic vibration parameters related to the non-H atom to which they are bonded. The crystallographic data for complexes **1·NO$_3$** and **2** are listed in Table 1, and selected bond lengths and bond angles are given in Table 2 and 3.

CCDC: 1907283, **1·NO$_3$**; 1907284, **2**.

Table 1　Crystallographic data for 1·NO$_3$ and 2

Complex	**1·NO$_3$**	**2**
Formula	$C_{38}H_{27}N_6O_3Ir$	$C_{38}H_{26}N_5Ir$
Formula weight	807.85	744.84
Crystal system	Orthorhombic	Monoclinic
Space group	*Pbca*	$P2_1/n$
T / K	296	296
a / nm	1.650 56(8)	1.036 46(7)
b / nm	1.390 24(7)	1.804 17(12)
c / nm	2.711 91(13)	1.606 89(11)
β / (°)		93.916 0(10)
V / nm^3	6.223 0(5)	2.997 8(4)
Z	8	4
D_c / (g·cm^{-3})	1.725	1.650
F(000)	3 184	1 464
GOF on F^2	1.035	1.015
R_1, wR_2 [$I>2\sigma(I)$]*	0.021 9, 0.072 6	0.031 6, 0.057 4
R_1, wR_2 (all data)	0.028 8, 0.077 4	0.063 4, 0.065 3
$(\Delta\rho)_{max}$, $(\Delta\rho)_{min}$ / (e·nm^{-3})	1 118, −609	836, −617

*$R_1=\sum||F_o|-|F_c||/\sum|F_o|$; $wR_2=[\sum w(F_o^2-F_c^2)^2/\sum w(F_o^2)^2]^{1/2}$.

Table 2　Selected bond lengths (nm) and bond angles (°) for 1·NO$_3$

Ir1-C1	0.200 8(3)	Ir1-N1	0.204 8(2)	N3-C32	0.133 0(4)
Ir1-C12	0.201 9(3)	Ir1-N3	0.214 2(2)	N4-C32	0.135 7(4)
Ir1-N2	0.203 9(2)	Ir1-N5	0.224 9(2)		
C1-Ir1-C12	84.05(12)	N1-Ir1-N3	89.19(9)	C18-N2-Ir1	116.3(2)
N2-Ir1-C1	95.19(10)	C1-Ir1-N5	167.73(10)	C32-N3-Ir1	114.8(2)
N2-Ir1-C12	80.42(11)	C12-Ir1-N5	105.82(11)	C33-N3-Ir1	138.3(2)
C1-Ir1-N1	81.10(10)	N2-Ir1-N5	93.67(9)	C31-N5-Ir1	113.3(2)
C12-Ir1-N1	94.34(11)	N1-Ir1-N5	90.74(9)	C23-N5-Ir1	128.4(2)
N2-Ir1-N1	173.91(10)	N3-Ir1-N5	75.65(9)	C2-C1-Ir1	128.8(2)
C1-Ir1-N3	94.98(11)	C11-N1-Ir1	126.2(2)	C6-C1-Ir1	113.7(2)
C12-Ir1-N3	176.14(11)	C7-N1-Ir1	115.1(2)		
N2-Ir1-N3	95.97(10)	C22-N2-Ir1	125.0(2)		

Table 3 Selected bond lengths (nm) and bond angles (°) for 2

Ir1-N1	0.204 1(3)	Ir1-N5	0.226 0(3)	N3-C32	0.134 1(5)
Ir1-N2	0.204 3(3)	Ir1-C1	0.201 8(4)	N4-C32	0.135 4(5)
Ir1-N4	0.212 3(3)	Ir1-C12	0.201 4(4)		
C12-Ir1-C1	84.55(15)	N2-Ir1-N4	89.15(12)	C18-N2-Ir1	115.2(3)
C12-Ir1-N1	95.00(16)	C12-Ir1-N5	170.39(14)	C32-N4-Ir1	115.9(3)
C1-Ir1-N1	80.63(15)	C1-Ir1-N5	104.31(13)	C38-N4-Ir1	140.0(3)
C12-Ir1-N2	80.83(16)	N1-Ir1-N5	90.18(12)	C31-N5-Ir1	112.8(2)
C1-Ir1-N2	95.05(15)	N2-Ir1-N5	94.51(12)	C23-N5-Ir1	129.7(3)
N1-Ir1-N2	174.30(13)	N4-Ir1-N5	75.93(12)	C2-C1-Ir1	129.8(3)
C12-Ir1-N4	95.51(14)	C11-N1-Ir1	125.0(3)	C6-C1-Ir1	114.2(3)
C1-Ir1-N4	175.75(14)	C7-N1-Ir1	115.9(3)		
N1-Ir1-N4	95.14(13)	C22-N2-Ir1	125.4(3)		

2 Results and discussion

2.1 Syntheses and structural transformation

Complex **1**·NO_3 were synthesized through the reaction of $[Ir(ppy)_2Cl]_2$ and qbiH in a CH_2Cl_2-CH_3OH solution at 50 ℃ for 24 hours, and followed by the anion exchange of Cl^- with NO_3^- for **1**·NO_3. In contrast, complex **2** was obtained by the reaction of $[Ir(ppy)_2Cl]_2$ and qbiH in the presence of K_2CO_3. Thus, an $[Ir(ppy)_2]^+$ unit is chelated by a qbi^- anion in complex **2**, while a neutral ligand qbiH in complex **1**·NO_3, which was confirmed by the crystal structures of these complexes.

Complexes **1**·NO_3 and **2** can interconvert in solution upon addition of an acid or a base, due to the structural transformation between ligand qbiH and ligand qbi^- (Scheme 1), which was supported by ^{1}H NMR spectra. After the $CDCl_3$ solution of **1**·NO_3 was fully mixed with a D_2O solution of NaOH, its ^{1}H NMR spectrum clearly changed to that of **2** (Fig.1). After adding some DCl in the $CDCl_3$ solution of **2**, although the measured ^{1}H NMR spectrum is different from that of **1**·NO_3 probably due to the influence of DCl, it is in agreement with the ^{1}H NMR spectrum of **1**·NO_3 in $CDCl_3$ containing DCl (Fig.2).

2.2 Crystal structures of 1·NO_3 and 2

In order to clarify the structures of complexes **1**·NO_3 and **2**, their crystal structures were measured. In complex **1**·NO_3, an $[Ir(ppy)_2]^+$ unit is coordinated by a neutral qbiH ligand (Fig.3). The resultant $[Ir(ppy)_2(qbiH)]^+$ cation connects a NO_3^- anion through hydrogen bond N4–H···O1–NO_2 (N4···O1 0.270 8(1) nm). In this cation, the Ir(Ⅲ) ion shows a distorted octahedral coordination geometry. Four of the six coordination sites around the Ir(Ⅲ) ion are occupied by two pyridine

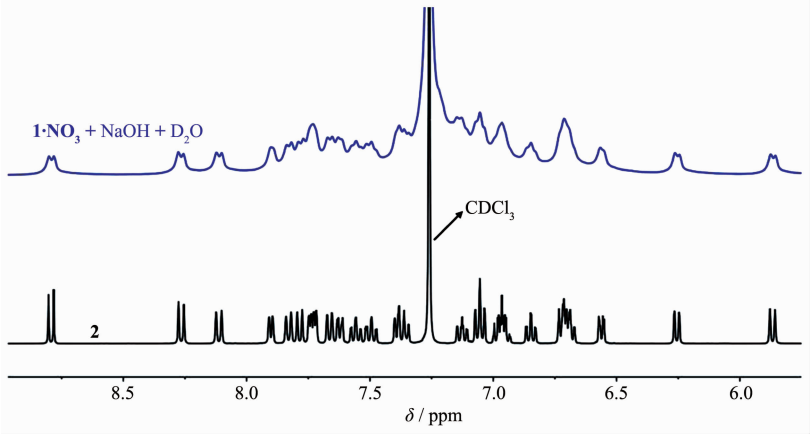

Fig.1 ^{1}H NMR spectra of **1**·NO_3 in $CDCl_3$ after adding NaOH and **2** in $CDCl_3$

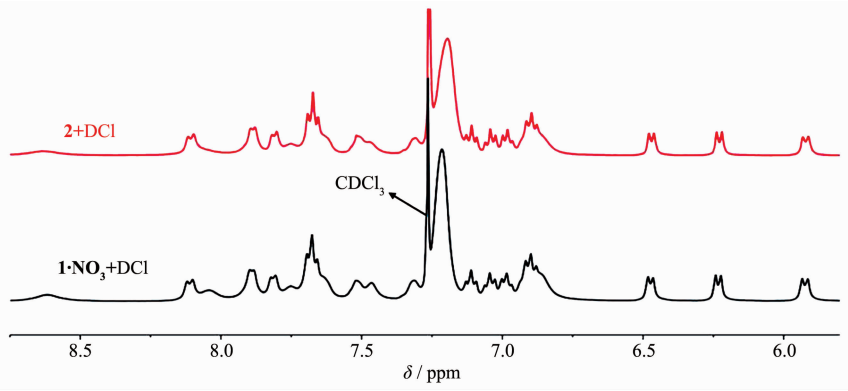

Fig.2　^{1}H NMR spectra of **2** in $CDCl_3$ after adding DCl and **1**·NO_3 in $CDCl_3$ containing DCl

nitrogen atoms (N1, N2) and two carbon atoms (C1, C12) from two nonequivalent cyclometalated ppy^- ligands. The remaining two coordination sites are filled with atoms N3 and N5 from a qbiH ligand. In the molecular structure of **1**·NO_3, two cyclometalated ppy^- ligands adopt the C,C-*cis* and N,N-*trans* arrangement as those in $[Ir(ppy)_2Cl]_2$[13]. Ligand qbiH is arranged with their nitrogen atoms N3 and N5 lying in the *trans*-position for σ-bond carbon atoms (C12 and C1) in the ppy^- ligands (*i.e.* N,C-*trans* arrangement), leading to much longer distances for Ir1-N3 bond (0.214 2(2) nm) and Ir1-N5 bond (0.224 9(2) nm) compared to Ir-$C(N)_{ppy}$ bonds (0.200 8(3)~0.204 8(2) nm)[14].

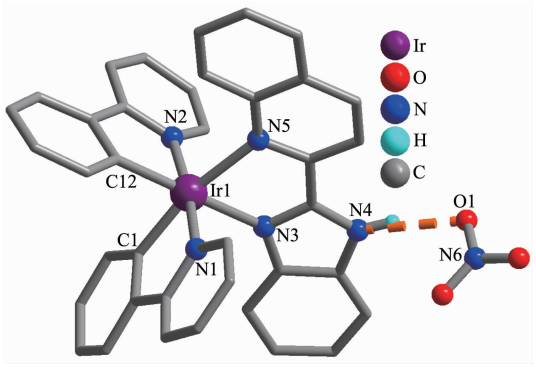

Orange dotted line indicating N–H···ONO_2 hydrogen bond; All H atoms attached to carbon atoms are omitted for clarity

Fig.3　Molecular structure of **1**·NO_3

Compared to **1**·NO_3, complex **2** is a neutral complex (Fig.4), in which a qbi^- anion uses its N4 and N5 atoms to coordinate with an $[Ir(ppy)_2]^+$ unit. In the molecular structure of **2**, ligands ppy^- and qbi^- adopt the same structural arrangements as those in **1**·NO_3, *i.e.* C,C-*cis*, N,N-*trans* and N,C-*trans* arrangements. The Ir-C(N) distances in **2** (0.2014(4)~0.2260(3) nm) are comparable to those in **1**·NO_3 (0.200 8(3)~0.224 9(2) nm).

Clearly, complexes **1**·NO_3 and **2** have different structures, a neutral ligand qbiH in the former while anion ligand qbi^- in the latter, which would lead to their distinct photophysical properties. Additionally, in the packing structures of both **1**·NO_3 and **2**, neighboring Ir(Ⅲ) fragments are held together by van der Waals interactions (Fig.S7 and S8), and there is no inter-molecular $\pi\cdots\pi$ stacking interactions as those in the reported complexes **1F**·PF_6 and **2F**. This indicates that the cyclometalated ligands ppy^- in both **1**·NO_3 and **2** can significantly affect the molecular arrangements of these complexes.

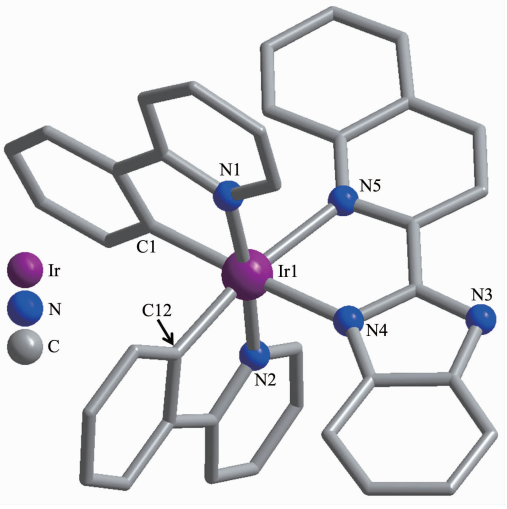

All H atoms attached to carbon atoms are omitted for clarity

Fig.4　Molecular structure of **2**

2.3　Electronic absorption spectra

The UV-Vis spectra of complexes **1**·NO_3 and **2**

were measured in CH_2Cl_2 at room temperature (Fig.5, Table 4). The complexes showed similar high-energy absorption bands at ~252 and 297 nm, which could be due to their ligand-centered (^{1}LC) transitions (ppy$^-$ and qbiH/qbi$^-$ ligands). However, the low-energy absorption bands of **2** (368 and 390 nm) show significant red shift compared to that of **1·NO$_3$** (368 nm). These low-energy absorption bands in the complexes are likely to be a combination of metal-to-ligand charge transfer (^{1}MLCT) and ligand-centered (^{1}LC) transition, because of their high extinction coefficients in a range of 1.5×10^4~2.0×10^4 L·mol^{-1}·cm^{-1} [5,14]. In addition, both **1·NO$_3$** and **2** exhibited weaker absorption tails towards 490 nm, which are mainly attributed to ^{3}MLCT absorptions in the complexes[15-16].

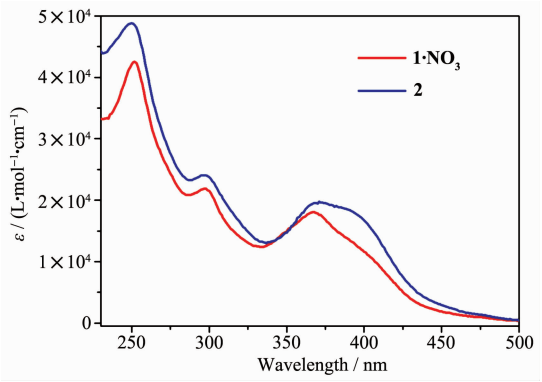

c=10 μmol·L^{-1}

Fig.5 UV-Vis absorption spectra of **1·NO$_3$** and **2** in CH_2Cl_2

Table 4 Photophysical data of 1·NO$_3$ and 2

Complex	Medium	λ_{abs} / nm	λ_{em} / nm	Lifetime / ns	Quantum yield / %
1·NO$_3$	CH_2Cl_2 (298 K)	252, 297, 368, 390 and a tail to 490	581	1 535	27.3
	EtOH-MeOH (77 K)	—	545 and 580	—	—
	Solid (298 K)	—	616	669 and 277	10.6
2	CH_2Cl_2 (298 K)	250, 297, 368, 390 and a tail to 490	574	1 716	23.3
	EtOH-MeOH (77 K)	—	543 and 577	—	—
	Solid (298 K)	—	598	3 129 and 664	11.5

2.4 Luminescence properties

We measured the luminescence spectra of both **1·NO$_3$** and **2** in CH_2Cl_2 at room temperature under the excitation with 398 nm (Fig.6). Compared to **1·NO$_3$** with an emission at 581 nm, complex **2** revealed a slightly blue-shifted emission at 574 nm, due to the fact that the deprotonated ligand qbi$^-$ leads to higher energy of MLCT (from Ir(Ⅲ) ion to ligand qbi$^-$). At 77 K, the complexes showed blue-shifted emissions with respect to their emissions at room temperature, occurring at 545 and 580 nm for **1·NO$_3$**, and 543 and 577 nm for **2** (Fig.S9, Table 4). This rigidochromism is characteristic of a CT character for the luminescence of these complexes[17-18]. In addition, the luminescence quantum yields (Φ) and the emission lifetimes (τ) of both **1·NO$_3$** and **2** were measured in degassed CH_2Cl_2 at room temperature, Φ=27.3% and τ=1 535 ns for **1·NO$_3$**, and Φ=23.3% and τ=1 716 ns for **2**.

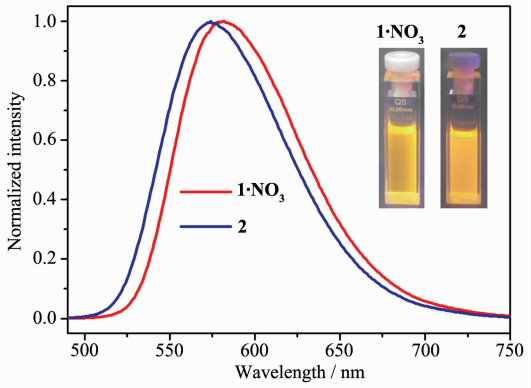

c=0.1 mmol·L^{-1}, λ_{ex}=398 nm

Fig.6 Luminescence spectra of **1·NO$_3$** and **2** in CH_2Cl_2

Clearly, complexes **1·NO$_3$** and **2** in CH_2Cl_2 have different luminescence, due to their different ancillary ligands (qbiH and qbi$^-$, respectively). On the other hand, compared to their analogous complexes **1F·PF$_6$** and **2F** (Scheme 1), both **1·NO$_3$** and **2** incorporate cyclometalated ligands ppy$^-$, which leads to their significantly different luminescence behaviors, mainly including the below three aspects. (i) The emission wavelengths of **1·NO$_3$** (581 nm) and **2** (574 nm) were longer than those of **1F·PF$_6$** (558 nm) and **2F** (546

nm), because the molecular structures of **1**·NO_3 and **2** have no electron-drawing fluorine group (Scheme 1). (ii) Complexes **1**·NO_3 and **2** revealed higher luminescence quantum yields (27.3% and 23.3%, respectively) than both **1F**·PF_6 (14%) and **2F** (3.2%). (iii) The quantum yield of **2F** (3.2%) was significantly lower than that of **1F**·PF_6 (14%), but the similar quantum yields for **1**·NO_3 (27.3%) and **2** (23.3%). This suggests that ligand qbi^- in complex **2** has less contribution to the excited state of this complex.

Although complexes **1**·NO_3 and **2** revealed the similar emission color in CH_2Cl_2 (Fig.6), they exhibited significantly different solid-state luminescence (Fig.7). A red emission at 611 nm was observed for **1**·NO_3, while an orange emission at 598 nm for complex **2**. The emissions of both **1**·NO_3 and **2** in solid state reveal significantly red shift compared to the corresponding emission in CH_2Cl_2, with $\Delta\lambda$=35 nm and 24 nm, respectively, which could be due to molecular aggregation in solid state[19]. For the solid-state samples of both **1**·NO_3 and **2**, we further measured their luminescence quantum yields and lifetimes. The complexes revealed similar solid-state luminescence quantum yield, Φ=10.6% for **1**·NO_3 and 11.5% for **2**. However, the solid-state emission lifetimes of **1**·NO_3 (τ_1=669 ns, 79% contribution and τ_2=277 ns, 21% contribution) are significantly shorter than those of 2 (τ_1=3 129 ns, 77% contribution and τ_2=664 ns, 23% contribution). The solid-state luminescence behaviors of **1**·NO_3 and **2** are clearly different from those of complexes **1F**·PF_6 (emissions at 542, 572 and 611 nm) and **2F** (emissions at 595 and 633 nm). This is in agreement with their distinct molecular structures and stacking structures (Scheme 1).

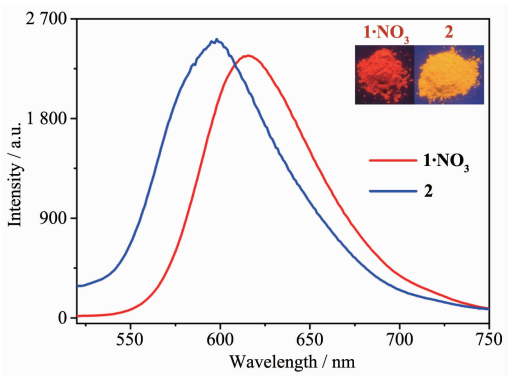

Inset: photographs of the complexes under 365 nm light

Fig.7　Luminescence spectra of **1**·NO_3 and **2** in solid state at room temperature

It is interesting that complexes **1**·NO_3 and **2** in solid state show acid/base-induced emission switching (Fig.8). Upon meeting the vapor of Et_3N, complex **1**·NO_3 changed its emission color from red to orange, indicating Et_3N-induced structural transition from $\mathbf{1}^+$ to **2** (*i.e.* from [Ir(ppy)(qbiH)]$^+$ to [Ir(ppy)(qbi)]). On the other hand, complex **2** showed emission-color change from orange to red upon meeting TFA vapor, which could be due to structural transition from **2** to $\mathbf{1}^+$. These experimental results indicate that solid-state complexes **1**·NO_3 and **2** can undergo TFA-/NEt_3-induced structural interconversion, leading to their emission color switching between red and yellow. It should be noted that the similar solid-state emission switching behavior has not been observed for **1F**·PF_6 and **2F**, which could be due to their close molecular stacking through $\pi\cdots\pi$ interactions (Fig.S1 and S2). Moreover, we found that the anion NO_3^- in complex **1**·NO_3 could be partly replaced by CF_3COO^- in TFA vapor, which was confirmed by the measurement of IR spectra (Fig.S14). After the treatment by TFA vapor, complex **1**·NO_3 showed two new peaks at 1 672 and 1 202 cm^{-1} from CF_3COO^- anion, indicating the replacement of NO_3^- by CF_3COO^-. Before and after meeting TFA vapor, complex **1**·NO_3 always revealed the absorption peaks of NO_3^- (1 425 and 842 cm^{-1}),

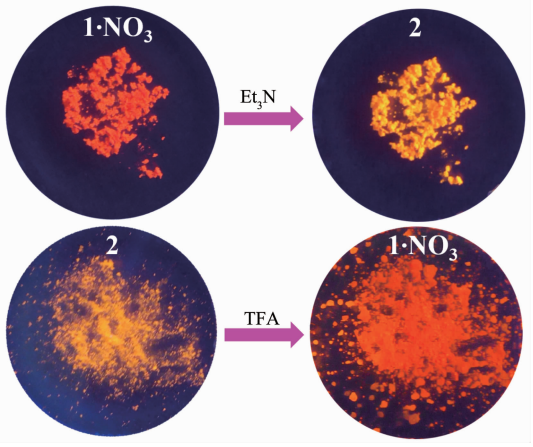

Fig.8　TFA-/Et_3N-induced emission switching for solid-sate **1**·NO_3 and **2** under 365 nm light at room temperature

suggesting that only a part of NO_3^- anions are replaced by CF_3COO^- anions.

3 Conclusions

In summary, we synthesized two new cyclometalated Ir(Ⅲ) complexes [Ir(ppy)(qbiH)]NO_3 (**1·NO$_3$**) and [Ir(ppy)(qbi)] (**2**). Their crystal structures indicate that an $[Ir(ppy)_2]^+$ unit is chelated by a neutral benzoimidazole-based ligand qbiH in **1·NO$_3$**, while anion ligand qbi^- in **2**. Neighboring Ir(Ⅲ) fragments in both **1·NO$_3$** and **2** are held together only by van der Waals interaction. The distinct molecular structures and packing structures between **1·NO$_3$** and **2** lead to their different luminescence both in CH_2Cl_2 and in solid state. In CH_2Cl_2, an emission at 581 nm with Φ= 27.3% was observed for **1·NO$_3$** and 574 nm with Φ= 23.3% for **2**. In solid state, complexes **1·NO$_3$** and **2** exhibit a red emission at 611 nm and an orange emission at 598 nm, respectively. Complexes **1·NO$_3$** and **2** revealed structural interconversion upon addition of acid/base (*i.e.* DCl/NaOD) in their $CDCl_3$ solution, which is assigned to acid/base-induced structural transformation between ligand qbiH and ligand qbi^-. This structural transformation can even occur in solid-state **1·NO$_3$** and **2**, probably due to the loose intermolecular stacking in the two complexes. Upon meeting Et_3N/TFA vapor, the solid-state samples of **1·NO$_3$** and **2** revealed luminescence switching between red emission and orange emission.

Supporting information is available at http://www.wjhxxb.cn

References:

[1] Murphy L, Congreve A, Palsson L O, et al. *Chem. Commun.*, **2010**,**46**:8743-8745

[2] (a)TONG Bi-Hai(童碧海), MEI Qun-Bo(梅群波), LI Zhi-Wen (李志文), et al. *Acta Chim. Sinica*(化学学报), **2012**,**70**: 2451-2456

(b)ZHOU Rui(周瑞), SONG Xin-Chao(宋新潮), TIAN Jie(田杰), et al. *Chinese Journal of Luminescence*(发光学报), **2010**,**31**:279-284

[3] Henwood A F, Hu Y, Sajjad M T, et al. *Chem. Eur. J.*, **2015**, **21**:19128-19135

[4] Hallett A J, Ward B D, Kariuki B M, et al. *J. Organomet. Chem.*, **2010**,**695**:2401-2409

[5] (a)Cao D K, Hu J S, Li M Q, et al. *Dalton Trans.*, **2015**,**44**: 21008-21015

(b)Gong D P, Gao T B, Cao D K, et al. *Dalton Trans.*, **2017**, **46**:275-286

[6] Rommel S A, Sorsche D, Rockstroh N, et al. *Eur. J. Inorg. Chem.*, **2015**:3730-3739

[7] He L, Ma D, Duan L, et al. *Inorg. Chem.*, **2012**,**51**:4502-4510

[8] Kappaun S, Eder S, Sax S, et al. *Eur. J. Inorg. Chem.*, **2007**: 4207-4215

[9] (a)Crosby G A, Demas J N. *J. Phys. Chem.*, **1971**,**75**:991-1024

(b)Brouwer A M. *Pure Appl. Chem.*, **2011**,**83**:2213-2228

[10]*SAINT, Program for Data Extraction and Reduction*, Siemens Analytical X-ray Instruments, Madison, WI, **1994-1996**.

[11]*SHELXTL, Reference Manual, Ver.*5.0, Siemens Industrial Automation, Analytical Instruments, Madison, WI, **1997**.

[12]Sheldrick G M. *Acta Crystallogr. Sect. A*: *Found. Crystallogr.*, **2008**,**A64**:112-122

[13]McGee K A, Mann K R. *Inorg. Chem.*, **2007**,**46**:7800-7809

[14]Marchi E, Sinisi R, Bergamini G, et al. *Chem. Eur. J.*, **2012**, **18**:8765-8773

[15]Mydlak M, Bizzarri C, Hartmann D, et al. *Adv. Funct. Mater.*, **2010**,**20**:1812-1820

[16]You Y, Lee S, Kim T, et al. *J. Am. Chem. Soc.*, **2011**,**133**: 18328-18342

[17]Tsuboyama A, Iwawaki H, Furugori M, et al. *J. Am. Chem. Soc.*, **2003**,**125**:12971-12979

[18]Kessler F, Costa R D, Censo D D, et al. *Dalton Trans.*, **2012**,**41**:180-191

[19]Yin S Y, Sun S S, Pan M, et al. *Inorg. Chem. Commun.*, **2017**,**83**:81-83